INTERNATIONAL JOURNAL FOR NUMERICAL METHODS IN ENGINEERING
Int. J. Numer. Meth. Engng 2008; **74**:871–893
Published online 18 October 2007 in Wiley InterScience (www.interscience.wiley.com). DOI: 10.1002/nme.2189

A geometrically exact thin membrane model—investigation of large deformations and wrinkling

Kerstin Weinberg[1,*,†] and Patrizio Neff[2]

[1]*Institute of Mechanics (MS2), Technical University of Berlin, Einsteinufer 5, 10587 Berlin, Germany*
[2]*AG6, Fachbereich Mathematik, Technische Universität Darmstadt, Schlossgartenstrasse 7, 64289 Darmstadt, Germany*

SUMMARY

We investigate a geometrically exact membrane model with respect to its capabilities in describing buckling and wrinkling. The concept is distinct from traditional ones by the introduction of an artificial viscosity related to an adjusted orthonormal frame (rotations). In this way our model is able to capture the detailed geometry of wrinkling while the balance of force equations remains elliptic throughout. The movement of rotations is given by a local evolution equation. We discuss the consistent linearization of the model and the local update of rotations. Numerical examples are presented, which demonstrate the effectiveness of the new model for predicting wrinkles in membranes undergoing large deformation. Copyright © 2007 John Wiley & Sons, Ltd.

Received 16 March 2007; Revised 10 August 2007; Accepted 14 August 2007

KEY WORDS: membranes; shells; thin films; energy minimization; viscoelasticity; transverse shear; tension-field theory; wrinkling; buckling

1. INTRODUCTION

Membrane-like structures are very diverse not only in nature but also in civil and mechanical engineering. In terms of structural mechanics, membranes are gossamer, i.e. flexible and thin-walled areal structures with a high load-bearing capacity and negligible bending resistance. In consequence, the equilibrium positions of membranes are characterized by a dominance of in-plane stresses and strains. Out-of-plane deformations are, of course, also observed in practice but they are usually understood as instabilities, e.g. folded, kinked or completely crashed (regions of) membranes.

*Correspondence to: Kerstin Weinberg, Institute of Mechanics (MS2), Technical University of Berlin, Einsteinufer 5, 10587 Berlin, Germany.
†E-mail: kerstin.weinberg@tu-berlin.de

Membrane-like structures are employed in many fields, e.g. air bags, balloons, ultra-light planes, solar sails of satellites or air beams and air cushions. Because of this huge range of applications there are numerous requests for a realistic description of the mechanical behavior of membranes. This can, in principle, be provided by means of classical shell theory. The different approaches toward elastic shell analysis are too numerous to list here, an illustrative review of today's state of the art provides [1] for a thorough mathematical analysis of the infinitesimal displacement shell theory, see [2] and references therein. However, because shell theories are designed for thin but not gossamer structures the computation of membranes with shell finite elements invokes all the theoretical and numerical difficulties that are encountered for the limit of characteristic thickness $h \to 0$ [3].

Therefore, more suitable for such flexible structures is the membrane theory, see [4] for an overview. Whereas a shell theory accounts for bending effects of the thin structures in classical membrane theory the bending stiffness is completely neglected. This *a priori* assumption renders the theory relatively simple, no (local) rotation of the membrane's mid-plane needs to be mapped. To develop their full load-bearing capacity a membrane requires a tensional state of stress; this fact is considered by the so-called tension field theories [5]. A traditional approach that goes back to the early 20th century is the introduction of a modified constitutive law to generate 'no-compression material' models [6, 7]. In a similar manner relaxed strain energy densities may avoid compressive stresses [8, 9]. More kinematically oriented approaches introduce a 'corrected' deformation gradient [10, 11], which allows also to include anisotropic and irreversible material laws. All these membrane theories have in common that they determine the load-bearing capacity of a membrane even in the presence of folds. Nonetheless, the detailed geometry, i.e. the actual position and amplitude of the folds remain undetermined.

However, instabilities like out-of-midplane deformation may also be of practical interest. An elastic membrane with no flexural rigidity will become wrinkled as soon as one of the principal stretches is non-positive. In general, three typical (local and in-plane) stress states may be distinguished. A membrane is *taut* when both principal stresses are tensile, a membrane is homogenously *wrinkled* when there is a uniaxial state of tensile stress, and, in the absence of tensile stresses the membrane is *slack*.

In this contribution we present results of a viscoelastic membrane model [12] which allows for the computation of all three membrane states in a continuous way. It has been derived by dimensional descent from a bulk model [13]. The model provides a geometrically exact finite deformation kinematic and is based on a modification of a viscoelastic strain energy density. Furthermore, the local well posedness of the suggested model has been shown, which sets it apart from practically all other geometrically exact membrane models [14]. Typically, membrane models are either accompanied by a complete loss of ellipticity in a slack state [15–17] or this loss of ellipticity is avoided by a quasiconvexification step, making it impossible to describe the geometry of the wrinkles [9, 18]. We will show here by examples that such a stress state may be captured by our (elliptic) model, too. Moreover, the model predicts the detailed geometry of the deformation. Another way to achieve the description of the detailed membrane geometry is based on dynamic relaxation, i.e. regarding the wrinkled equilibrium as a long time limit of a damped dynamical problem, see [19].

Remark on notation: We work here in the context of non-linear, finite viscoelasticity and consider a time period $t \in [0, T]$. In the following $\omega \subset \mathbb{R}^2$ denotes the flat referential domain of the membrane with smooth (Lipschitz continuous) boundary $\partial\omega$, the characteristic thickness is $h > 0$.

DOI: 10.1002/nme

For vectors $a, b \in \mathbb{R}^3$ we denote with $\langle a, b \rangle$ the scalar product with associated vector norm $\|a\| = \langle a, a \rangle$. By $\mathbb{M}^{n\times m}$ the set of linear mappings $\mathbb{R}^n \mapsto \mathbb{R}^m$ is identified. In particular, $\mathbb{M}^{3\times 3}$ is the set of real 3×3 second-order tensors, written with capital letters. The standard Euclidean scalar product on $\mathbb{M}^{3\times 3}$ is given by $\langle X, Y \rangle = \mathrm{tr}[XY^{\mathrm{T}}]$, and thus the Frobenius tensor norm is $\|X\|^2 = \langle X, X \rangle$. The identity tensor on $\mathbb{M}^{3\times 3}$ will be denoted by $\mathbb{1}$, so that $\mathrm{tr}[X] = \langle X, \mathbb{1} \rangle$. For $w \in \mathbb{M}^{3\times 2}$ and $X_3 \in \mathbb{R}^3$ we employ the notation $(w|X_3) \in \mathbb{M}^{3\times 3}$ to write the matrix composed of w and the (third) column vector of tensor X. Likewise, $(x|y|z)$ is the matrix composed of vectors $x, y, z \in \mathbb{R}^3$.

Moreover, we adopt here the usual abbreviations of Lie-group theory, i.e. $\mathrm{GL}(3) := \{X \in \mathbb{M}^{3\times 3} \,|\, \det X \neq 0\}$ is the general linear group and $\mathrm{SO}(3) := \{X \in \mathrm{GL}(3) \,|\, X^{\mathrm{T}}X = \mathbb{1},\ \det X = 1\}$ is the subgroup of orthogonal tensors.

2. THE FINITE-STRAIN-VISCOELASTIC MEMBRANE MODEL

The spatial deformation of a thin-walled structure $\phi_s : \omega \times (-h/2, h/2) \to \mathbb{R}^3$ can be viewed as being composed of the motion of the midsurface $m : \omega \subset \mathbb{R}^2 \mapsto \mathbb{R}^3$ and of the motion of the director (initially) orthogonal to the midsurface. Presuming a plane initial state and with the coordinates indicated in Figure 1 we write for the displacement of the midsurface $u : \omega \subset \mathbb{R}^2 \mapsto \mathbb{R}^3$, such that $m(x, y) = (x, y, 0)^{\mathrm{T}} + u(x, y)$. The membrane model presented here uses the polar decomposition of the deformation gradient into a continuum rotation R and a symmetric stretch tensor U. Let us write the polar decomposition in the form $F = RU = \mathrm{polar}(F)\,U$ with $R = \mathrm{polar}(F)$ being the orthogonal part of the deformation gradient F and $R \in \mathrm{SO}(3)$. The out-of-plane component of this continuum rotation, $R(x, y).e_3$, is the natural choice for the director of the midsurface $m(x, y)$ consistent with small strains in the three-dimensional model. In consequence, and with an additional

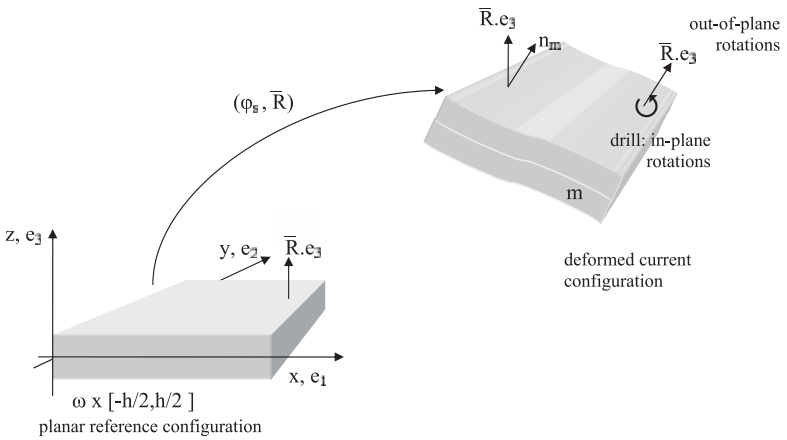

Figure 1. The three-dimensional membrane kinematics incorporating viscoelastic transverse shear ($\overline{R}_3 \neq \mathbf{n}_m$) and instantaneous thickness stretch ($\varrho_m \neq 1$).

DOI: 10.1002/nme

factor $\varrho_m \in \mathbb{R}$ to account for a varying plate thickness, the *spatial motion* of an initially plane membrane can be written as

$$\phi_s(x, y, z) = m(x, y) + z\varrho_m(x, y)\, R(x, y).e_3 \tag{1}$$

The exact expression of ϱ_m has been derived in [12, 14] from plate kinematics under the usual assumption of plane stress state with the result

$$\varrho_m(x, y) = 1 - \frac{\lambda}{2\mu+\lambda}[\langle(\nabla m|0), R(x, y)\rangle - 2] \tag{2}$$

where λ, μ are the Lame moduli and $\nabla m \in \mathbb{M}^{3\times 2}$ is the deformation gradient of the midsurface with $m_x = (m_{1,x}, m_{2,x}, m_{3,x})^{\mathrm{T}}$, $m_y = (m_{1,y}, m_{2,y}, m_{3,y})^{\mathrm{T}}$.

The basic idea of our viscoelastic membrane model is the introduction of an *additional* field of independently evolving viscoelastic rotations $\overline{R} \in \mathrm{SO}(3)$. These rotations $\overline{R}$ are thought of as being physically meaningful but not exact continuum rotations R. With $\overline{R}_3 \equiv \overline{R}(x, y).e_3$ denoting the corresponding out-of-plane component the dimensional reduction of a three-dimensional continuum solid to a geometrically exact membrane model results in a deformation gradient of the form

$$F = (\nabla m|\varrho_m \overline{R}_3) \tag{3}$$

The rotational part in function (2) changes accordingly, and, $\varrho_m : \mathbb{M}^{3\times 2} \times \mathrm{SO}(3) \mapsto \mathbb{R}$ accounts for a thickness stretch of the membrane, i.e. the thickness decreases for increasing membrane stretch.

For the membrane material we consider a classical isotropic strain energy density $W(F) = W(U) = \mu\|U - \mathbb{1}\|^2 + (\lambda/2)\,\mathrm{tr}[U - \mathbb{1}]^2$ in terms of the Biot strain tensor $U - \mathbb{1}$. Replacing the continuum rotations, $R = \mathrm{polar}(F)$, with the field of independently evolving viscoelastic rotations, $\overline{R} \in \mathrm{SO}(3)$, defines a non-symmetric second-order tensor $\overline{U} = \overline{R}^{\mathrm{T}} F$. Since $\overline{U}$ is not any more positive-definite symmetric we substitute the positive-definite classical stretch in the strain energy by the best approximation of $\overline{U}$ in terms of positive-definite tensors [20] given by $\mathrm{sym}(\overline{U})$.[‡] Thus, the elastic energy density turns into

$$W(F, \overline{R}) = \frac{\mu}{4}\|F^{\mathrm{T}}\overline{R} + \overline{R}^{\mathrm{T}}F - 2\mathbb{1}\|^2 + \frac{\lambda}{8}\,\mathrm{tr}[F^{\mathrm{T}}\overline{R} + \overline{R}^{\mathrm{T}}F - 2\mathbb{1}]^2 \tag{4}$$

Moreover, let $W^{\mathrm{ext}}(m)$ be the linear work of applied external forces with f_b being the resultant body forces and f_s the resultant surface traction and let $g_{\mathrm{d}} : [0, T] \times \omega \mapsto \mathbb{R}^3$ denote the prescribed Dirichlet boundary conditions for the membrane

$$\begin{aligned} W^{\mathrm{ext}}(m) &= \int_\omega \langle f_b, m\rangle \,\mathrm{d}\omega - \int_{\gamma_s} \langle f_s, m\rangle \,\mathrm{ds} \\ m_{|\gamma_0}(t, x, y) &= g_{\mathrm{d}}(t, x, y), \quad x, y \in \gamma_0 \subset \partial\omega \end{aligned} \tag{5}$$

[‡]$\mathrm{sym}(\overline{U})$ is the best approximation of $\overline{U}$ in the set of positive-definite symmetric tensors as long as $\langle F.\xi, \overline{R}.\xi\rangle \geqslant 0$ for all $\xi \in \mathbb{R}^3$.

DOI: 10.1002/nme

The membrane problem in a variational formulation then reads: find the deformation of the midsurface $m:[0,T]\times\omega\mapsto\mathbb{R}^3$ and the independent local viscoelastic rotation $\overline{R}:[0,T]\times\omega\mapsto \mathrm{SO}(3,\mathbb{R})$ such that

$$\int_\omega hW(F,\overline{R})\,\mathrm{d}\omega-\int_\omega\langle f_b,m\rangle\,\mathrm{d}\omega-\int_{\gamma_s}\langle f_s,m\rangle\,\mathrm{ds}\mapsto\min \tag{6}$$

w.r.t. m at fixed rotation $\overline{R}$.

The field of local viscoelastic rotation follows an *evolution equation*

$$\frac{\mathrm{d}}{\mathrm{dt}}\overline{R}(t)=v^+\cdot\mathrm{skew}(B)\cdot\overline{R}(t)\quad\text{with } v^+:=\frac{1}{\eta}v^+(F,\overline{R})\ \text{ and }\ B=F\overline{R}^{\mathrm{T}} \tag{7}$$

Here $v^+\in\mathbb{R}^+$ represents a scalar-valued function introducing an *artificial viscosity* and η plays the role of an *artificial relaxation time* (with units [s]). The evolution equation (7) and parameter v^+ are introduced into the model to preserve ellipticity of the force balance. Physically, one may imagine the viscoelastic rotation $\overline{R}$ as *shadowing* the exact continuum rotation in a viscous sense.

The *stresses* generated *in the membrane* are the derivative of the strain energy density w.r.t the corresponding deformation tensor. Consequently, we obtain here for the first Piola–Kirchhoff stress tensor

$$S(F,\overline{R}):=D_FW(F,\overline{R})=\mu\overline{R}(F^{\mathrm{T}}\overline{R}+\overline{R}^{\mathrm{T}}F-2\cdot\mathbb{1})+\lambda\langle F^{\mathrm{T}}\overline{R}-\mathbb{1},\mathbb{1}\rangle\cdot\overline{R} \tag{8}$$

where F is the reconstructed deformation gradient (3). Then the Cauchy stresses as well as other stress tensors follow by the well-known transformation rules [21]. Note that the Cauchy stresses are in general non-symmetric (due to the independent field of rotations $\overline{R}$) but turn out to be close to symmetry by our choice of a small artificial viscosity.

Before we proceed with a temporal and spatial discretization of the presented model we add here some remarks to associate our model with other approaches of dimensional reduction.

Remark 2.1

Note that for the reduced term $\widehat{F}=(\nabla m|\overline{R}_3)$ instead of (3) the elastic energy can be written in fact as

$$\begin{aligned}W(F,\overline{R})&=\mu\|\mathrm{sym}(F^{\mathrm{T}}\overline{R}-\mathbb{1})\|^2+\frac{\lambda}{2}\,\mathrm{tr}[\mathrm{sym}(F^{\mathrm{T}}\overline{R}-\mathbb{1})]^2\\&=\mu\|\mathrm{sym}(\widehat{F}^{\mathrm{T}}\overline{R}-\mathbb{1})\|^2+\frac{\mu\lambda}{(2\mu+\lambda)}\,\mathrm{tr}[\mathrm{sym}(\widehat{F}^{\mathrm{T}}\overline{R}-\mathbb{1})]^2\end{aligned} \tag{9}$$

showing the characteristic apparent change of the Lamé moduli μ,λ for the two-dimensional structure due to the plain stress state. Here, $\mu\lambda/(2\mu+\lambda)$ is half of the harmonic mean of μ and $\lambda/2$. Observe that it is not expedient to use $\widehat{F}$ in the condensed form (9) since in the coupled evolution Equation (7) it is F of Equation (3) which appears.

Remark 2.2

The three-dimensional deformation (1) can be reconstructed through

$$\phi_s(x,y,z):=m(x,y)+z\varrho_m(x,y)\,\overline{R}(x,y).e_3\quad\text{and}\quad\nabla\boldsymbol{\phi}_s(x,y,0)=(\nabla m|\varrho_m\,\overline{R}_3) \tag{10}$$

DOI: 10.1002/nme

Inserting the ansatz for the reconstructed deformation (10) into the underlying continuum model and enforcing traction-free boundary conditions at the upper and lower face of the membrane in an averaged sense determines the analytical expression for ϱ_m used in $(3)_2$. We note that it is not possible to prescribe boundary conditions for the rotations $\overline{R}$ in this viscoelastic membrane formulation.

Remark 2.3
Due to the underlying isotropy, model (6) approaches in the vanishing viscosity limit $v^+ \to \infty$ (same as zero relaxation time limit $\eta \to 0$ or complete relaxation, long time limit) formally the intrinsic two-dimensional membrane-shell problem

$$\int_\omega h W_\infty(U(\nabla m|\mathbf{n}_m))\,\mathrm{d}\omega - W^{\mathrm{ext}}(m) \mapsto \text{stat.} \quad \text{w.r.t. } m$$

$$W_\infty(U) = \mu\|U-\mathbb{1}\|^2 + \frac{\mu\lambda}{2\mu+\lambda}\,\mathrm{tr}[U-\mathbb{1}]^2 \tag{11}$$

with $\mathbf{n}_m$ being the unit normal on the parameterized membrane surface. Thus, U is the classical symmetric elastic stretch and $U-\mathbb{1}$ is the elastic Biot strain tensor

$$U = U(\nabla m|\mathbf{n}_m) = \begin{pmatrix} \sqrt{\nabla m^{\mathrm{T}}\nabla m} & 0 \\ 0 & 1 \end{pmatrix} \tag{12}$$

Problem (11) is a geometrically exact equilibrium membrane model for small elastic strains and finite deformations in the *classical* sense, i.e. with no extra internal process. The transition from (6) to (11) in the formal relaxation limit $\eta \to 0$, however, is not entirely trivial since it is not just the replacement of the independent rotation $\overline{R}$ by the continuum rotation $R = (\nabla m|\mathbf{n}_m)U^{-1}$. Moreover, note the subtle change from global minimization to a stationarity requirement only. As well, it must be noted that the elastic equilibrium energy $W_\infty(U)$ is non-quasiconvex and non-elliptic w.r.t. $\nabla m \in \mathbb{M}^{3\times 2}$ but it is convex in the classical symmetric stretch U. Currently, there are no mathematical theorems available establishing the existence of minimizers or equilibria solutions based directly on W_∞. In this sense, the viscoelastic formulation (6) provides a physical *regularization* of the occurring *loss of ellipticity* in the more classical formulation (11).

3. DISCRETIZATION OF THE MODEL

3.1. Temporal discretization

Let us now consider a fully implicit time-discretized version of model (6). In principle, the simplest method for one time step is the following staggered scheme: let $(m^{n-1}, \overline{R}^{n-1})$ be the given solution for the deformation of the midsurface and the rotations at time t_{n-1}. Now, compute the new solution

DOI: 10.1002/nme

$(m^n, \overline{R}^n) \in \mathbb{V}$ at time t_n such that[§]

$$\int_\omega hW(F^n, \overline{R}^n)\,\mathrm{d}\omega - W^{\mathrm{ext},n}(m^n) \mapsto \min \tag{13}$$

w.r.t. m^n at fixed $\overline{R}^n$ and with strain energy density function (4). The current deformation gradient $F^n = F(t_n)$ is

$$F^n = (\nabla m^n | \varrho_m^n \overline{R}_3^n) \quad \text{with } \varrho_m^n = 1 - \frac{\lambda}{2\mu+\lambda}[\langle (\nabla m^n | 0), \overline{R}^n \rangle - 2]$$

and the current boundary conditions are

$$m^n_{|\gamma_0}(t_n, x, y) = g_\mathrm{d}(t_n, x, y), \quad x, y \in \gamma_0 \subset \partial\omega \tag{14}$$

The evolution equation for the rotations is now mapped by a *local exponential update*. This implies that $\overline{R}^n = \overline{R}^n(\nabla m^n)$ solves the following highly non-linear problem:

$$\overline{R}^n = \exp(\Delta t v_n^+ \operatorname{skew}(F^n \overline{R}^{n,\mathrm{T}})) \cdot \overline{R}^{n-1} \quad \text{with } v_n^+ = \frac{1}{\eta}(1 + \|\operatorname{skew} F^n \overline{R}^{n,\mathrm{T}}\|)^2 \tag{15}$$

By the properties of logarithmic and exponential mapping it can easily be shown that (15) converges to (7) for the limit $\Delta t \to 0$. We will come back to this in Section 4.

Furthermore, for each load and time step $\Delta t = [t_{n-1}, t_n]$ we compute the new solution $m^n, \overline{R}^n$ by an iteration $m^{n,j}, \overline{R}^{n,j}$ with the understanding that

$$\lim_{j\to\infty} m^{n,j} = m^n, \quad \lim_{j\to\infty} \overline{R}^{n,j} = \overline{R}^n \tag{16}$$

Remark (Start values)
The iteration (we employ here a classical Newton scheme) is very sensitive as far as proper start values for the current time step are concerned. This is all the more the case since our non-linear problem admits multiple stationary solutions, e.g. uniform compression *versus* bulging out. In order to capture the 'interesting' minimizing solution we proceed as follows: first, we compute locally the orthogonal part of the reconstructed deformation gradient in the previous time step,

$$\overline{R}^n_{-1} := \operatorname{polar}(\nabla m^{n-1} | \varrho_m^{n-1} \overline{R}_3^{n-1}) \tag{17}$$

Then we solve the following (modified) minimization problem for $m^{n,0}$:

$$\int_\omega hW(F^{n,0}, \overline{R}^n_{-1})\,\mathrm{d}\omega - W^{\mathrm{ext},n}(m^{n,0}) \mapsto \min \quad \text{w.r.t. } m^{n,0} \text{ at fixed } \overline{R}^n_{-1} \tag{18}$$

[§]We abbreviate here $\mathbb{V} = H_0^{1,2}(\omega, \mathbb{R}^3; \gamma_0) \times L^2(\omega, \mathrm{SO}(3))$, where the space $H_0^{1,2}(\omega, \mathbb{R}^3; \gamma_0)$ is the set of all functions $m : \omega \subset \mathbb{R}^2 \mapsto \mathbb{R}^3$ which have square-integrable weak derivatives and vanish on $\gamma_0 \subset \partial\omega$ in the sense of traces and $L^2(\omega, \mathrm{SO}(3))$ is the set of all measurable fields of proper rotations $R : \omega \mapsto \mathrm{SO}(3)$. We employ the standard notation of Sobolev spaces, i.e. $L^2(\Omega)$, $H^{1,2}(\Omega)$, $H_0^{1,2}(\Omega)$, indifferently for scalar-valued functions as well as for vector-valued and tensor-valued functions.

DOI: 10.1002/nme

We now set

$$\overline{R}^{n,0} = \mathrm{polar}(\nabla m^{n,0}|_{\varrho_m}(\nabla m^{n,0}, \overline{R}^n_{-1})\overline{R}^n_{-1}.e_3) \tag{19}$$

and take the pair $(m^{n,0}, \overline{R}^{n,0})$ as initial elastic trial solution for a subsequent global Newton iteration.

3.2. Spatial discretization

The finite element discretization of problem (6) considers discrete subspaces of the continuous solution spaces for the membrane's deformation. Thus, the *discrete problem* reads: find the deformation of the midsurface of the membrane and the independent local viscoelastic rotation $(m_h, \overline{R}_h)$: $[0,T]\times\mathbb{V}_h$ such that

$$\int_\omega h W(F(m_h), \overline{R}_h)\,\mathrm{d}\omega - W^{\mathrm{ext}}(m_h) \mapsto \min \tag{20}$$

w.r.t. m_h at fixed rotation $\overline{R}_h$.

The discrete space $\mathbb{V}_h$ is the space of $\mathscr{T}$-piecewise polynomials based on a regular triangulation $\mathscr{T}$ of ω in (closed) triangles or parallelograms. We assume that the triangulation matches the domain exactly, i.e. $\cup\mathscr{T}=\omega$ and two distinct elements T_1 and T_2 in $\mathscr{T}$ are either disjoint, or $T_1\cap T_2$ is a complete edge or a common vertex of both (there are no hanging nodes). Let $\mathscr{P}_k(\mathscr{T})$ be the linear space of $\mathscr{T}$-piecewise polynomials of degree $\leqslant k$, and let $\mathscr{P}^0_k(\mathscr{T})$ denote the continuous discrete functions in $\mathscr{P}_k(\mathscr{T})$ with homogeneous boundary values, i.e.

$$\mathscr{P}_k(\mathscr{T}) := \{u_h \in L^2(\omega):\ \forall T\in\mathscr{T},\ u_h|_T \in \mathscr{P}_k(T)\} \quad \text{and} \quad \mathscr{P}^0_k(\mathscr{T}) := \mathscr{P}_k(\mathscr{T})\cap H^1_0(\omega) \tag{21}$$

If $T\in\mathscr{T}$ is a triangle, $\mathscr{P}_k(T)$ denotes the space of polynomials of total degree $\leqslant k$; while $\mathscr{P}_k(T)$ denotes the space of polynomials of partial degree $\leqslant k$ if T is a parallelogram. Consequently, the discrete subspace of the deformation of the midsurface identifies with $\mathscr{P}^0_{k+1}(\mathscr{T})^3$ for any non-negative integer k. We apply here $k=0$ but an extension of the subspace, i.e. an (adaptive) mesh refinement, may raise computational efficiency, cf. [22, 23]. In every time step Δt the spatial discretization reads

$$\mathbb{V}_h = \mathscr{P}^0_1(\mathscr{T})^3 \times \mathscr{P}_0(\mathscr{T})^{3\times 3} \tag{22}$$

In the following we omit the subindex h for readability.

3.3. Weak form of the thin membrane model

To formulate the finite element equations the weak form of problem (6), i.e. the principle of virtual work, is derived here. Let $\delta m :\in \mathbb{M}^{3\times 2}$ denote the virtual displacement of the midsurface with $\delta m \in H^{1,2}_0(\omega, \mathbb{R}^3; \gamma_0)$. Then we obtain for fixed rotations $\overline{R}\equiv\overline{R}^n$

$$\int_\omega h\,\langle D_{\nabla m}[W(F^n, \overline{R})], \nabla(\delta m)\rangle\,\mathrm{d}\omega - W^{\mathrm{ext},n}(\delta m) = 0 \tag{23}$$

where we used the linearity of W^{ext}. Performing the differentiation w.r.t. ∇m this is equivalent to

$$\int_\omega h\langle D_F W(F^n, \overline{R}), (\nabla(\delta m)| - \frac{\lambda}{2\mu+\lambda}\langle(\nabla(\delta m)|0), \overline{R}\rangle\,\overline{R}_3)\rangle\,\mathrm{d}\omega - W^{\mathrm{ext},n}(\delta m) = 0 \tag{24}$$

DOI: 10.1002/nme

For the strain energy density function (4) it holds that for an arbitrary three-dimensional increment, $H \in \mathbb{M}^{3\times 3}$, the differential is given by

$$\langle D_F W(F,\overline{R}), H\rangle = \mu\langle F^{\mathrm{T}}\overline{R}+\overline{R}^{\mathrm{T}}F-2\cdot\mathbb{1}, \overline{R}^{\mathrm{T}}H\rangle + \lambda\langle F^{\mathrm{T}}\overline{R}-\mathbb{1},\mathbb{1}\rangle\cdot\langle\overline{R}^{\mathrm{T}}H,\mathbb{1}\rangle \tag{25}$$

Therefore, taking as increment

$$H\equiv\delta F^n = (\nabla(\delta m)|\delta\varrho_m^n\,\overline{R}_3^n) \quad \text{with } \delta\varrho_m^n = -\frac{\lambda}{2\mu+\lambda}\langle(\nabla(\delta m)|0),\overline{R}^n\rangle \tag{26}$$

we infer that

$$\delta F^n = (\nabla(\delta m)| - \frac{\lambda}{2\mu+\lambda}\langle(\nabla(\delta m)|0),\overline{R}^n\rangle\,\overline{R}_3^n) \tag{27}$$

and we obtain for (24) the expression

$$\begin{aligned}\int_\omega h[&\mu\langle F^{\mathrm{T},n}\overline{R}+\overline{R}^{\mathrm{T}}F^n-2\cdot\mathbb{1}, \overline{R}^{\mathrm{T}}(\nabla(\delta m)| - \frac{\lambda}{2\mu+\lambda}\langle(\nabla(\delta m)|0),\overline{R}^n\rangle\,\overline{R}_3^n)\rangle\\ &+\lambda\langle F^{\mathrm{T},n}\overline{R}-\mathbb{1},\mathbb{1}\rangle\cdot\langle\overline{R}^{\mathrm{T}}(\nabla(\delta m)| - \frac{\lambda}{2\mu+\lambda}\langle(\nabla(\delta m)|0),\overline{R}^n\rangle\,\overline{R}_3^n),\mathbb{1}\rangle]\,\mathrm{d}\omega\\ &-W^{\mathrm{ext},n}(\delta m)=0\end{aligned} \tag{28}$$

To obtain the weak form *consistent* with the local exponential update the rotations $\overline{R}$ need to be replaced with $\overline{R}^n(\nabla m^n)$ according to Equation (15). Finally, the consistent weak form of problem (6) reads with (27)

$$\begin{aligned}\int_\omega h[&\mu\,\langle F^{\mathrm{T},n}\overline{R}^n(\nabla m^n)+\overline{R}^{\mathrm{T},n}(\nabla m^n)F^n-2\cdot\mathbb{1}, \overline{R}^{\mathrm{T},n}(\nabla m^n)\cdot\delta F^n\rangle\\ &+\lambda\,\langle F^{\mathrm{T},n}\overline{R}^n(\nabla m^n)-\mathbb{1},\mathbb{1}\rangle\cdot\langle\overline{R}^{\mathrm{T},n}(\nabla m^n)\cdot\delta F^n,\mathbb{1}\rangle]\,\mathrm{d}\omega - W^{\mathrm{ext},n}(\delta m)=0\end{aligned} \tag{29}$$

where it should be emphasized again that F^n is itself a non-linear function of ∇m^n,

$$F^n = (\nabla m^n|\varrho_m(\nabla m^n,\overline{R}^n(\nabla m^n))\overline{R}^n(\nabla m^n).e_3)$$

Let us remark that by our approach (20)–(22) the rotations are discontinuous along the element edges. Therefore, the rotations jump over elemental interfaces and we expect and observe kinks of the shell's midsurface. The exact positions of these kinks in the numerical solution depend, to a certain extent, on the triangulation.

4. THE IMPLICIT LOCAL EXPONENTIAL UPDATE FOR THE ROTATIONS IN THREE DIMENSIONS

This section is devoted to a detailed discussion of the key feature of our model, the local exponential update of the rotations $\overline{R}(t)$. To this end let us first consider the following local, non-linear

DOI: 10.1002/nme

subproblem: given an arbitrary, fully three-dimensional deformation history $F \in C^1(\mathbb{R}^+, \mathrm{GL}^+(3))$, determine a time-dependent rotation $R \in C^1(\mathbb{R}^+, \mathrm{SO}(3))$ such that

$$\frac{\mathrm{d}}{\mathrm{dt}} R(t) = v^+ \cdot \mathrm{skew}(F(t) R^{\mathrm{T}}) \cdot R(t), \quad R(0) = R_0 \in \mathrm{SO}(3) \tag{30}$$

with

$$v^+ = \frac{1}{\eta}(1 + \|\mathrm{skew}(F(t) R^{\mathrm{T}}(t))\|)^2$$

This problem is at first sight independent of (13). In [13] it has been shown that for *fixed in time* F the solution $R(t)$ converges asymptotically to the continuum rotation $R = \mathrm{polar}(F)$. We first validate this general analytical result for our numerical algorithm.

In Section 3.1 we proposed to integrate the local evolution equation (30) numerically with an *implicit exponential update*, i.e. we solve the time-discretized version (15). Set now for readability

$$\overline{R} \equiv \overline{R}^{n-1}, \quad X \equiv \overline{R}^{n}, \quad F \equiv F^n, \quad B \equiv F \overline{R}^{\mathrm{T}} = F^n \overline{R}^{n-1,\mathrm{T}} \tag{31}$$

and let us define a function $\gamma(s)$ with $s = \|\mathrm{skew}(F \overline{R}^{\mathrm{T}})\|$ and

$$\gamma(s) = \frac{1}{\eta}(1+s)^2, \quad \gamma'(s) = \frac{2(1+s)}{\eta} \tag{32}$$

Then the proposed implicit local update for the rotations consists of solving

$$X = \exp(\Delta t \gamma(\|\mathrm{skew}(F X^{\mathrm{T}})\|)\, \mathrm{skew}(F X^{\mathrm{T}})) \cdot \overline{R} \tag{33}$$

for $X \in \mathrm{SO}(3)$. If we set $X = Q \cdot \overline{R}$, we need to solve

$$Q = \exp(\Delta t \gamma(\|\mathrm{skew}(F \overline{R}^{\mathrm{T}} Q^{\mathrm{T}})\|)\, \mathrm{skew}(F \overline{R}^{\mathrm{T}} Q^{\mathrm{T}})) \tag{34}$$

where $Q = \overline{R}^{n} \overline{R}^{n-1,\mathrm{T}}$ is the time-incremental change of the rotations in one step. Set now $Q = \exp(A)$ for some $A \in \mathfrak{so}(3)$ by the local bijectivity of the exponential function. This turns (34) into

$$\exp(A) = \exp(\Delta t \gamma(\|\mathrm{skew}(F \overline{R}^{\mathrm{T}} \exp(A)^{\mathrm{T}})\|)\, \mathrm{skew}(F \overline{R}^{\mathrm{T}} \exp(A)^{\mathrm{T}})) \tag{35}$$

for the new unknown $A \in \mathfrak{so}(3)$. Since $\exp : \mathfrak{so}(3) \mapsto \mathrm{SO}(3)$ is bijective on a large ball around zero (cf. (44)) we have equivalently and still exact

$$A = \Delta t \gamma(\|\mathrm{skew}(B \exp(A)^{\mathrm{T}})\|)\, \mathrm{skew}(B \exp(A)^{\mathrm{T}}) \tag{36}$$

The solution of (36) at given B will be denoted by A^{ex}. The non-linear equation (36) will here be solved with a *local Newton iteration*. If A^{ex} is determined, then $\overline{R}^{n} = X = \exp(A^{\mathrm{ex}}) \overline{R}^{n-1}$.

Since we expect the incremental change in one time step to be small anyhow (equivalent to small A) we may approximate $\exp(A)^{\mathrm{T}} \approx \mathbb{1} - A$ and introduce this approximation into (36). This leads us to consider

$$\begin{aligned} A \;&=\; \Delta t \gamma(\|\mathrm{skew}(B(\mathbb{1} - A))\|)\, \mathrm{skew}(B(\mathbb{1} - A)) \\ &\Rightarrow A = \Delta t \gamma\, \mathrm{skew}(B) - \Delta t \gamma\, \mathrm{skew}(B A) \end{aligned} \tag{37}$$

DOI: 10.1002/nme

Assuming for the moment that γ is already given this equation has a unique solution A whenever $A \mapsto A + \Delta t \gamma \operatorname{skew}(B\,A)$ is strictly monotone, i.e. $\forall A \in \mathfrak{so}(3)$:

$$\langle A + \Delta t \gamma \operatorname{skew}(B\,A), A \rangle > 0 \tag{38}$$

Since

$$\begin{aligned} \langle A + \Delta t \gamma \operatorname{skew}(B\,A), A \rangle &= \|A\|^2 + \Delta t \gamma \langle B\,A, A \rangle \\ &\geqslant \|A\|^2 - \Delta t \gamma \|A\|^2 \|B\| = \|A\|^2 [1 - \Delta t \gamma \|B\|] \end{aligned} \tag{39}$$

we obtain a useful bound on the size of *time step* Δt

$$\Delta t \gamma < \|B\|^{-1} \tag{40}$$

which ensures condition (38) and implies algorithmically that (36) has a unique solution. This bound will be used in the implementation throughout. Concluding let us emphasize that the actual computation of A is performed with Equation (36), the linearized version $(37)_1$ is only applied to derive the time step bound (40).

4.1. The start value for the local Newton iteration

At given $F, \overline{R}$ we want to solve Equation (33). In view of the local relaxation limit $R = \operatorname{polar}(F)$, a good start value X_0 for X should be given by $X^0 = \operatorname{polar}(F)$. Since the final Newton method will be based on Equation (36) and since $X = Q\,\overline{R} = \exp(A)\overline{R}$ we consider

$$\begin{aligned} \operatorname{polar}(F) \;&=\; X^0 = Q^0\,\overline{R} = \exp(A^0)\,\overline{R} \\ &\Rightarrow A^0 = \log(\operatorname{polar}(F)\overline{R}^{\mathrm{T}}) = \log(\operatorname{polar}(F^n)\,\overline{R}^{n-1,\mathrm{T}}) \in \mathfrak{so}(3) \end{aligned} \tag{41}$$

where the matrix-logarithm on rotations $\log : \mathrm{SO}(3) \mapsto \mathfrak{so}(3)$ is well defined up to absolute values of rotation angles less than π [24].

4.2. The local Newton iteration for the rotational update

In this paragraph we derive the incremental linearization of the local exponential update in detail. According to (36) we have to solve the non-linear matrix equation

$$A = \Delta t\, v^+(B \exp(A)^{\mathrm{T}}) \cdot \operatorname{skew}(B \exp(A)^{\mathrm{T}}) \tag{42}$$

with $v^+(B \exp(A)^{\mathrm{T}}) = \gamma(\|\operatorname{skew}(B \exp(A)^{\mathrm{T}})\|)$ and function (32). A local Newton step corresponding to the non-linear equation (36) is obtained by inserting $A^k + \Delta A$ into (36) in lieu of A and expanding it with respect to the increment ΔA up to first order. Set for the moment $A = A^k + \Delta A$. Then

$$\begin{aligned} A^k + \Delta A &= \Delta t\, v^+(B \exp(A^k + \Delta A)^{\mathrm{T}}) \cdot \operatorname{skew}(B \exp(A^k + \Delta A)^{\mathrm{T}}) \\ &= \Delta t\, (v^+(B \exp(A^k)^{\mathrm{T}}) + D_A[v^+(B \exp(A^k)^{\mathrm{T}})].\Delta A + \cdots) \\ &\quad (\operatorname{skew}(B \exp(A^k)^{\mathrm{T}}) + \operatorname{skew}(B[D \exp(A^k).\Delta A]^{\mathrm{T}})) \end{aligned} \tag{43}$$

DOI: 10.1002/nme

Let us first collect some facts from Lie-group theory. We define the matrix exponential function

$$\exp:\mathfrak{so}(3)\mapsto \mathrm{SO}(3),\quad \exp(X)=\sum_{i=1}^{\infty}\frac{1}{i!}X^i \tag{44}$$

This function is bijective on a large ball around $0\in\mathfrak{so}(3)$, more precisely, for $\|X\|^2=-\mathrm{tr}[X^2]<2\pi^2$ or equivalently, if $\|\mathrm{axl}(X)\|<\pi$ [24]. Let us also introduce the *adjoint operator*

$$\mathrm{ad}:\mathfrak{so}(3)\mapsto \mathrm{Lin}(\mathfrak{so}(3),\mathfrak{so}(3)),\quad \mathrm{ad}(X).Y=[X,Y]=XY-YX \tag{45}$$

The analytical form of the differential of the matrix exponential function can be written as [24]

$$D\exp(X).H=\exp(X)\cdot\left[\sum_{i=1}^{\infty}\frac{1}{i!}(-\mathrm{ad}(X))^{i-1}\right].H \tag{46}$$

with the series expanded to

$$\begin{aligned}\left[\sum_{i=1}^{\infty}\frac{1}{i!}(-\mathrm{ad}(X))^{i-1}\right].H&=\left[\mathbb{1}-\frac{1}{2}\mathrm{ad}(X)+\frac{1}{3!}\mathrm{ad}(X)^2+\cdots\right].H\\&=H-\frac{1}{2}\mathrm{ad}(X).H+\frac{1}{3!}\mathrm{ad}(X).(\mathrm{ad}(X).H)+\cdots\end{aligned} \tag{47}$$

For commutating pairs $(X,H)\in\mathfrak{so}(3)\times\mathfrak{so}(3)$ we have $\mathrm{ad}(X).H=0$ and we recover the classical derivative formula $D\exp(X).H=\exp(X)\cdot H$. For brevity let us define an operator $P_l(\mathrm{ad}(X)).H\in\mathfrak{so}(3)$ with

$$P_l(\mathrm{ad}(X)).H=\left[\sum_{i=1}^{l}\frac{1}{i!}(-\mathrm{ad}(X))^{i-1}\right].H \tag{48}$$

The index refers to the order of approximation $l\in\mathbb{N}$ in (47), throughout the paper we employ $l=2$. An approximation of the differential is obtained by using

$$D_{.,l}\exp(X).H=\exp(X)\cdot P_l(\mathrm{ad}(X)).H \tag{49}$$

Since $\exp(A)^{\mathrm{T}}\cdot\exp(A)=\mathbb{1}$ for all $A\in\mathfrak{so}(3)$[¶] it holds that $\exp(A)^{\mathrm{T}}\cdot D\exp(A).H\in\mathfrak{so}(3)$ for arbitrary $H\in\mathfrak{so}(3)$. This feature is shared by the approximate formula to any order of approximation, since

$$\exp(A)^{\mathrm{T}}\cdot D_{.,l}\exp(A).H=\exp(A)^{\mathrm{T}}\cdot\exp(A)\cdot P_l(\mathrm{ad}(A)).H=P_l(\mathrm{ad}(A)).H \tag{50}$$

With formulas (44)–(49) we evaluate Equation (43) to

$$\begin{aligned}&A^k+\Delta A\\&\quad\approx\Delta t\,v^+(B\exp(A^k)^{\mathrm{T}})\,\mathrm{skew}(B\exp(A^k)^{\mathrm{T}})+\Delta t\,v^+(B\exp(A^k)^{\mathrm{T}})\,\mathrm{skew}(B[D\exp(A^k).\Delta A]^{\mathrm{T}})\\&\qquad+\Delta t\,(D_A[v^+(B\exp(A^k)^{\mathrm{T}})].\Delta A)\cdot\mathrm{skew}(B\exp(A^k)^{\mathrm{T}})\end{aligned}$$

[¶] $\exp(A)^{\mathrm{T}}=\exp(-A)$ and $\exp(-A)\exp(A)=\exp(-A+A)=\exp(0)=\mathbb{1}$ for all $A\in\mathfrak{so}(3)$.

DOI: 10.1002/nme

$$
\begin{aligned}
&= \Delta t v^+(B\exp(A^k)^{\mathrm{T}})\,\mathrm{skew}(B\exp(A^k)^{\mathrm{T}}) \\
&+ \Delta t v^+(B\exp(A^k)^{\mathrm{T}})\,\mathrm{skew}(B[P_l(\mathrm{ad}(A^k)).\Delta A]^{\mathrm{T}}\exp(A^k)^{\mathrm{T}}) \\
&+ \Delta t (D_A[v^+(B\exp(A^k)^{\mathrm{T}})].\Delta A)\cdot \mathrm{skew}(B\exp(A^k)^{\mathrm{T}}) \qquad (51)
\end{aligned}
$$

The linear approximation for the non-linear viscosity term $\gamma(\|\mathrm{skew}(B\exp(A^k)^{\mathrm{T}})\|)$ is given by

$$
\begin{aligned}
&D_A[\gamma(\|\mathrm{skew}(B\exp(A^k)^{\mathrm{T}})\|)].\Delta A \\
&= \gamma'(\|\mathrm{skew}(B\exp(A^k)^{\mathrm{T}})\|)\left\langle \frac{\mathrm{skew}(B\exp(A^k)^{\mathrm{T}})}{\|\mathrm{skew}(B\exp(A^k)^{\mathrm{T}})\|}, \mathrm{skew}(B\cdot[D\exp(A^k).\Delta A]^{\mathrm{T}})\right\rangle \\
&\approx \gamma'(\|\mathrm{skew}(B\exp(A^k)^{\mathrm{T}})\|)\left\langle \frac{B^{\mathrm{T}}\mathrm{skew}(B\exp(A^k)^{\mathrm{T}})}{\|\mathrm{skew}(B\exp(A^k)^{\mathrm{T}})\|}, [D_{\cdot,l}\exp(A^k).\Delta A]^{\mathrm{T}}\right\rangle \\
&= \gamma'(\|\mathrm{skew}(B\exp(A^k)^{\mathrm{T}})\|)\left\langle \frac{B^{\mathrm{T}}\mathrm{skew}(B\exp(A^k)^{\mathrm{T}})}{\|\mathrm{skew}(B\exp(A^k)^{\mathrm{T}})\|}, [\exp(A^k)P_l(\mathrm{ad}(A^k)).\Delta A]^{\mathrm{T}}\right\rangle \\
&= -\gamma'(\|\mathrm{skew}(B\exp(A^k)^{\mathrm{T}})\|)\left\langle \frac{B^{\mathrm{T}}\mathrm{skew}(B\exp(A^k)^{\mathrm{T}})\exp(A^k)}{\|\mathrm{skew}(B\exp(A^k)^{\mathrm{T}})\|}, P_l(\mathrm{ad}(A^k)).\Delta A\right\rangle \qquad (52)
\end{aligned}
$$

Combining this with the former computation, we obtain

$$
\begin{aligned}
&A^k + \Delta A \\
&\approx \Delta t\gamma(\|\mathrm{skew}(B\exp(A^k)^{\mathrm{T}})\|)\,\mathrm{skew}(B\exp(A^k)^{\mathrm{T}}) \\
&\quad -\Delta t\gamma(\|\mathrm{skew}(B\exp(A^k)^{\mathrm{T}})\|)\mathrm{skew}(B[P_l(\mathrm{ad}(A^k)).\Delta A]\exp(A^k)^{\mathrm{T}}) \\
&\quad -\Delta t\gamma'(\|\mathrm{skew}(B\exp(A^k)^{\mathrm{T}})\|)\left\langle \frac{B^{\mathrm{T}}\mathrm{skew}(B\exp(A^k)^{\mathrm{T}})\exp(A^k)}{\|\mathrm{skew}(B\exp(A^k)^{\mathrm{T}})\|}, P_l(\mathrm{ad}(A^k)).\Delta A\right\rangle \\
&\quad \cdot\mathrm{skew}(B\exp(A^k)^{\mathrm{T}}) \qquad (53)
\end{aligned}
$$

Abbreviate now

$$
S^{n,k} = \mathrm{skew}(B^n\exp(A^k)^{\mathrm{T}}), \quad N^{\mathrm{ex}} = \|S^{n,k}\| \qquad (54)
$$

and set for the *local residuum* (the defect of (36))

$$
\mathrm{Res}(B, A^k) = A^k - \Delta t\gamma(\|\mathrm{skew}(B\exp(A^k)^{\mathrm{T}})\|)\,\mathrm{skew}(B\exp(A^k)^{\mathrm{T}}) \qquad (55)
$$

The local Newton method consists in iterating $A^{k+1} := A^k + \Delta A$ until $\|\mathrm{Res}^k\| \leqslant$ tolerance. Using these abbreviations yields the *linear matrix equation* for $\Delta A \in \mathfrak{so}(3)$

$$
\begin{aligned}
\mathrm{Res}(B, A^k) + \Delta A = &-\Delta t\,\gamma(N^{\mathrm{ex}})\,\mathrm{skew}(B[P_l(\mathrm{ad}(A^k)).\Delta A]\exp(A^k)^{\mathrm{T}}) \\
&-\Delta t\frac{\gamma'(N^{\mathrm{ex}})}{N^{\mathrm{ex}}}\langle B^{\mathrm{T}}S\exp(A^k), P_l(\mathrm{ad}(A^k)).\Delta A\rangle\cdot S \qquad (56)
\end{aligned}
$$

DOI: 10.1002/nme

or

$$\Delta A+\Delta t\gamma(N^{\mathrm{ex}})\,\mathrm{skew}(B[P_l(\mathrm{ad}(A^k)).\Delta A]\exp(A^k)^{\mathrm{T}})$$
$$+\Delta t\frac{\gamma'(N^{\mathrm{ex}})}{N^{\mathrm{ex}}}\langle B^{\mathrm{T}}S\exp(A^k),\,P_l(\mathrm{ad}(A^k)).\Delta A\rangle\cdot S=-\mathrm{Res}(B,A^k) \tag{57}$$

Now we reduce this equation to a linear vector equation for $\Delta a=\mathrm{axl}(\Delta A)$ applying on both sides of the equation the operator

$$\mathrm{axl}:\mathfrak{so}(3)\mapsto\mathbb{R}^3,\quad \mathrm{axl}\begin{pmatrix}0&\alpha&\beta\\-\alpha&0&\gamma\\-\beta&-\gamma&0\end{pmatrix}=\begin{pmatrix}-\gamma\\\beta\\-\alpha\end{pmatrix} \tag{58}$$

with inverse $\mathrm{anti}:\mathbb{R}^3\mapsto\mathfrak{so}(3)$. This yields

$$\mathrm{axl}(\Delta A)+\Delta t\gamma(N^{\mathrm{ex}})\,\mathrm{axl}(\mathrm{skew}(B[P_l(\mathrm{ad}(A^k)).\Delta A]\exp(A^k)^{\mathrm{T}}))$$
$$+\Delta t\frac{\gamma'(N^{\mathrm{ex}})}{N^{\mathrm{ex}}}\langle B^{\mathrm{T}}S\exp(A^k),\,P_l(\mathrm{ad}(A^k)).\Delta A\rangle\cdot\mathrm{axl}(S)=-\mathrm{axl}(\mathrm{Res}(B,A^k)) \tag{59}$$

or

$$\Delta a+\Delta t\gamma(N^{\mathrm{ex}})\,\mathrm{axl}(\mathrm{skew}(B[P_l(\mathrm{ad}(A^k)).\mathrm{anti}(\Delta a)]\exp(A^k)^{\mathrm{T}}))$$
$$+\Delta t\frac{\gamma'(N^{\mathrm{ex}})}{N^{\mathrm{ex}}}\langle B^{\mathrm{T}}S\exp(A^k),\,P_l(\mathrm{ad}(A^k)).\mathrm{anti}(\Delta a)\rangle\cdot\mathrm{axl}(S)=-\mathrm{axl}(\mathrm{Res}(B,A^k)) \tag{60}$$

The linear operators on the left-hand side, which act on Δa will be expressed with matrix operations applied to $\Delta a\in\mathbb{R}^3$. The corresponding matrix representation is easily obtained by putting into the ith column the image of the ith base vector $e_i\in\mathbb{R}^3$ under the action of the linear operator. Thus, we obtain

$$\begin{pmatrix}\Delta a_1\\\Delta a_2\\\Delta a_3\end{pmatrix}+\Delta t\gamma(N^{\mathrm{ex}})\begin{pmatrix}\mathrm{axl}(\mathrm{skew}(B[P_l(\mathrm{ad}(A^k)).\mathrm{anti}(e_1)]\exp(A^k)^{\mathrm{T}}))\\\mathrm{axl}(\mathrm{skew}(B[P_l(\mathrm{ad}(A^k)).\mathrm{anti}(e_2)]\exp(A^k)^{\mathrm{T}}))\\\mathrm{axl}(\mathrm{skew}(B[P_l(\mathrm{ad}(A^k)).\mathrm{anti}(e_3)]\exp(A^k)^{\mathrm{T}}))\end{pmatrix}^{\mathrm{T}}\begin{pmatrix}\Delta a_1\\\Delta a_2\\\Delta a_3\end{pmatrix}$$
$$+\Delta t\frac{\gamma'(N^{\mathrm{ex}})}{N^{\mathrm{ex}}}\begin{pmatrix}\langle B^{\mathrm{T}}S\exp(A^k),\,P_l(\mathrm{ad}(A^k)).\mathrm{anti}(e_1)\rangle\cdot\mathrm{axl}(S)\\\langle B^{\mathrm{T}}S\exp(A^k),\,P_l(\mathrm{ad}(A^k)).\mathrm{anti}(e_2)\rangle\cdot\mathrm{axl}(S)\\\langle B^{\mathrm{T}}S\exp(A^k),\,P_l(\mathrm{ad}(A^k)).\mathrm{anti}(e_3)\rangle\cdot\mathrm{axl}(S)\end{pmatrix}^{\mathrm{T}}\begin{pmatrix}\Delta a_1\\\Delta a_2\\\Delta a_3\end{pmatrix}$$
$$=-\mathrm{axl}(\mathrm{Res}(B,A^k)) \tag{61}$$

DOI: 10.1002/nme

Then we compute the increment $\Delta A = \mathrm{anti}(\Delta a)$ and the final local rotation X follows by $X = \exp(A^{\mathrm{ex}}) \cdot \overline{R}$ with the local solution

$$A^{k+1} := A^k + \Delta A, \quad A^{\mathrm{ex}} = \lim_{k \to \infty} A^k \tag{62}$$

In view of $S \in \mathfrak{so}(3)$ we have $\|S\| = \sqrt{2}\sqrt{S_{12}^2 + S_{13}^2 + S_{23}^2}$.

4.3. Convergence of the local Newton iteration

In the preceding section we proposed a numerically robust implicit exponential update as a consistent discretization for the evolution equation for the rotations that preserves the Lie-group structure of SO(3) on the discrete level. This scheme takes advantage of the underlying property that the quadratic minimization problem is uniquely solvable at given $\overline{R}^n$. In order to validate this update numerically we studied carefully the convergence properties of the evolution equation (30). Exemplarily, we present here results choosing a deformation gradient $\hat{F}$ such that we know the exact rotation $\hat{R}$ immediately. Take

$$\begin{aligned}
\hat{F}(\varphi) &= \hat{R}(\varphi) \cdot \hat{U}(\varphi) \\
\hat{R}(\varphi) &= \begin{pmatrix} 1 & 0 & 0 \\ 0 & \cos(\varphi) & \sin(\varphi) \\ 0 & -\sin(\varphi) & \cos(\varphi) \end{pmatrix} \\
\hat{U}(\varphi) &= \begin{pmatrix} (1+\frac{1}{2}\sin(\varphi))^2 & 0 & \sin^2(\varphi) \\ 0 & \dfrac{1}{1+\frac{1}{2}\sin(\varphi)} & 0 \\ \sin^2(\varphi) & 0 & \dfrac{1}{1+\frac{1}{2}\sin(\varphi)} \end{pmatrix}
\end{aligned} \tag{63}$$

The computed rotation R^n is now compared with the exact rotation for different values of viscosity η. To this end we monitor the error

$$e = \| R^{n\mathrm{T}} \hat{R} - \mathbb{1} \| \tag{64}$$

In Figure 2 error (64) is plotted *versus* the total time for $\varphi = \pi/3$ in Equation (63). Here and below the start value for the rotational update is $R^0 = \mathbb{1}$. The error decreases rapidly for all values of viscosity η; however, the larger the value of η the slower the rate of convergence. This result nicely reflects the special feature of our proposed membrane model (6). However, the numerical computation of exponential and logarithmic matrix mappings is sensitive and has a relatively large inherent numerical error.

Results for different sizes of time step Δt are not displayed here. For every value of viscosity η the curves computed for all time increments would lay on top of each other; the actual size of step Δt has no influence on the accuracy of the solution.

DOI: 10.1002/nme

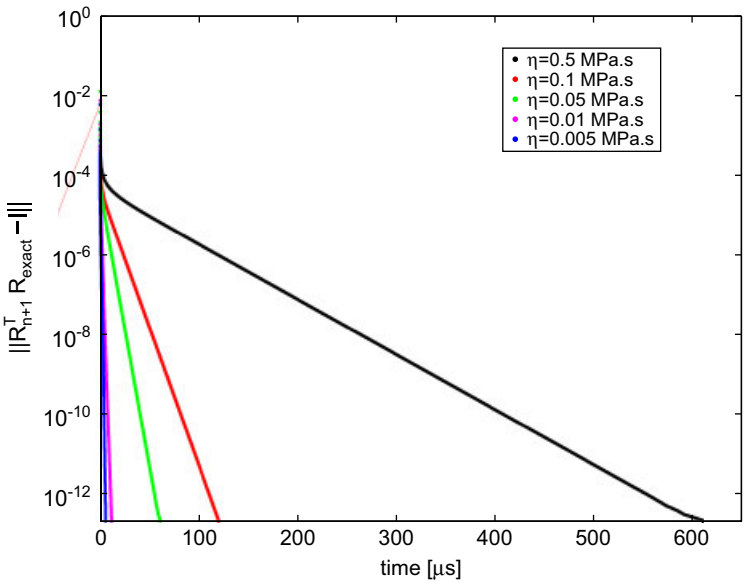

Figure 2. Error of the rotational update $\|R^{n\mathrm{T}}\hat{R} - I\|$ *versus* time for different values of viscosity η and a constant time step Δt.

4.4. Local response tangent for A^{ex} in three dimensions

We conclude this section with the differential of the local response of the material with respect to the rotations. Let $A^{\mathrm{ex}}(F^n\overline{R}^{n-1,\mathrm{T}})$ solve (36). Then the exponential update is characterized by

$$\overline{R}^n(F^n) = \exp(A^{\mathrm{ex}}(F^n\overline{R}^{n-1,\mathrm{T}}))\cdot\overline{R}^{n-1} \tag{65}$$

The exact differential of this local response, which is needed in a subsequent global Newton step, is given by

$$D_F\overline{R}(F).H = [D\exp(A^{\mathrm{ex}}(F\overline{R}^{n-1,\mathrm{T}})).[DA^{\mathrm{ex}}(F\overline{R}^{n-1,\mathrm{T}}).(H\overline{R}^{n-1,\mathrm{T}})]]\cdot\overline{R}^{n-1} \tag{66}$$

cf. (31) for the notation. Since A^{ex} satisfies Equation (36)

$$A(B) = \Delta t\,\gamma(\|\mathrm{skew}(B\exp(A(B))^{\mathrm{T}})\|)\cdot\mathrm{skew}(B\exp(A(B))^{\mathrm{T}}), \quad B := F^n\overline{R}^{n-1,\mathrm{T}} \tag{67}$$

we obtain by differentiating w.r.t. $B\in\mathbb{M}^{3\times3}$ and for any increment $H\in\mathbb{M}^{3\times3}$

$$\begin{aligned}
DA(B).H &\approx \Delta t\,D_B[v^+(B\exp(A(B)^{\mathrm{T}})\cdot\mathrm{skew}(B\exp(A(B))^{\mathrm{T}})].H\\
&= \Delta t\,Dv^+(B\exp(A(B))^{\mathrm{T}}).[H\exp(A(B))^{\mathrm{T}} + B[D\exp(A(B)).[DA(B).H]]^{\mathrm{T}}]\\
&\quad\times\mathrm{skew}(B\exp(A(B))^{\mathrm{T}}) + \Delta t\,v^+(B\exp(A(B))^{\mathrm{T}})\\
&\quad\times\mathrm{skew}([H\exp(A(B))^{\mathrm{T}} + B[D\exp(A(B)).[DA(B).H]]^{\mathrm{T}}])\\
&= \Delta t\,Dv^+(B\exp(A(B))^{\mathrm{T}}).[H\exp(A(B))^{\mathrm{T}}
\end{aligned}$$

DOI: 10.1002/nme

$$+B[P_l(\mathrm{ad}(A(B))).[DA(B).H]]^{\mathrm{T}}\exp(A(B))^{\mathrm{T}}]$$
$$\times\mathrm{skew}(B\exp(A(B))^{\mathrm{T}})+\Delta t v^{+}(B\exp(A(B))^{\mathrm{T}})$$
$$\times\mathrm{skew}([H\exp(A(B))^{\mathrm{T}}+B[P_l(\mathrm{ad}(A(B))).[DA(B).H]]^{\mathrm{T}}\exp(A(B))^{\mathrm{T}}])$$

Set $\mathfrak{H}=DA^{\mathrm{ex}}(B).H$ where $\mathfrak{H}\in\mathfrak{so}(3)$ and abbreviate

$$S^{\mathrm{ex}}=\mathrm{skew}(B\exp(A(B))^{\mathrm{T}}),\quad N^{\mathrm{ex}}=\|S^{\mathrm{ex}}\| \tag{68}$$

This yields

$$\mathfrak{H}=\Delta t\frac{\gamma'(N^{\mathrm{ex}})}{N^{\mathrm{ex}}}\langle S^{\mathrm{ex}},[H\exp(A(B))^{\mathrm{T}}-B[P_l(\mathrm{ad}(A(B))).\mathfrak{H}]\exp(A(B))^{\mathrm{T}}]\rangle\cdot S^{\mathrm{ex}}$$
$$+\Delta t\gamma(N^{\mathrm{ex}})\cdot\mathrm{skew}([H\exp(A(B))^{\mathrm{T}}-B[P_l(\mathrm{ad}(A(B))).\mathfrak{H}]\exp(A(B))^{\mathrm{T}}]) \tag{69}$$

since $P_l(\mathrm{ad}(A(B))).\mathfrak{H}\in\mathfrak{so}(3)$. Define as well

$$\mathrm{Res}^{\mathrm{ex}}(H,A(B))=\Delta t\frac{\gamma'(N^{\mathrm{ex}})}{N^{\mathrm{ex}}}\langle S^{\mathrm{ex}},[H\exp(A(B))^{\mathrm{T}}]\rangle\cdot S^{\mathrm{ex}}+\Delta t\gamma(N^{\mathrm{ex}})\cdot\mathrm{skew}([H\exp(A(B))^{\mathrm{T}}]) \tag{70}$$

Thus (with $A(B)=A^{\mathrm{ex}}$)

$$\mathfrak{H}+\Delta t\frac{\gamma'(N^{\mathrm{ex}})}{N^{\mathrm{ex}}}\langle S^{\mathrm{ex}},B[P_l(\mathrm{ad}(A(B))).\mathfrak{H}]\exp(A^{\mathrm{ex}})^{\mathrm{T}}\rangle\cdot S^{\mathrm{ex}}$$
$$+\Delta t\gamma(N^{\mathrm{ex}})\cdot\mathrm{skew}(B[P_l(\mathrm{ad}(A^{\mathrm{ex}})).\mathfrak{H}]\exp(A^{\mathrm{ex}})^{\mathrm{T}})=\mathrm{Res}^{\mathrm{ex}}(H,A^{\mathrm{ex}}) \tag{71}$$

As before, we transform this linear matrix equation into a corresponding vector format for $x=\mathrm{axl}(\mathfrak{H})\in\mathbb{R}^3$:

$$x+\Delta t\frac{\gamma'(N^{\mathrm{ex}})}{N^{\mathrm{ex}}}\langle S^{\mathrm{ex}},B[P_l(\mathrm{ad}(A^{\mathrm{ex}})).\mathrm{anti}(x)]\exp(A^{\mathrm{ex}})^{\mathrm{T}}\rangle\cdot\mathrm{axl}(S^{\mathrm{ex}})$$
$$+\Delta t\gamma(N^{\mathrm{ex}})\cdot\mathrm{axl}(\mathrm{skew}(B[P_l(\mathrm{ad}(A^{\mathrm{ex}})).\mathrm{anti}(x)]\exp(A^{\mathrm{ex}})^{\mathrm{T}}))=\mathrm{axl}(\mathrm{Res}^{\mathrm{ex}}(H,A^{\mathrm{ex}})) \tag{72}$$

Thus

$$\begin{pmatrix}x_1\\x_2\\x_3\end{pmatrix}+\Delta t\gamma(N^{\mathrm{ex}})\begin{pmatrix}\mathrm{axl}(\mathrm{skew}(B[P_l(\mathrm{ad}(A^{\mathrm{ex}})).\mathrm{anti}(e_1)]\exp(A^{\mathrm{ex}})^{\mathrm{T}}))\\\mathrm{axl}(\mathrm{skew}(B[P_l(\mathrm{ad}(A^{\mathrm{ex}})).\mathrm{anti}(e_2)]\exp(A^{\mathrm{ex}})^{\mathrm{T}}))\\\mathrm{axl}(\mathrm{skew}(B[P_l(\mathrm{ad}(A^{\mathrm{ex}})).\mathrm{anti}(e_3)]\exp(A^{\mathrm{ex}})^{\mathrm{T}}))\end{pmatrix}^{\mathrm{T}}\begin{pmatrix}x_1\\x_2\\x_3\end{pmatrix}$$
$$+\Delta t\frac{\gamma'(N^{\mathrm{ex}})}{N^{\mathrm{ex}}}\begin{pmatrix}\langle B^{\mathrm{T}}S^{\mathrm{ex}}\exp(A^{\mathrm{ex}}),P_l(\mathrm{ad}(A^{\mathrm{ex}})).\mathrm{anti}(e_1)\rangle\cdot\mathrm{axl}(S^{\mathrm{ex}})\\\langle B^{\mathrm{T}}S^{\mathrm{ex}}\exp(A^{\mathrm{ex}}),P_l(\mathrm{ad}(A^{\mathrm{ex}})).\mathrm{anti}(e_2)\rangle\cdot\mathrm{axl}(S^{\mathrm{ex}})\\\langle B^{\mathrm{T}}S^{\mathrm{ex}}\exp(A^{\mathrm{ex}}),P_l(\mathrm{ad}(A^{\mathrm{ex}})).\mathrm{anti}(e_3)\rangle\cdot\mathrm{axl}(S^{\mathrm{ex}})\end{pmatrix}^{\mathrm{T}}\begin{pmatrix}x_1\\x_2\\x_3\end{pmatrix}$$
$$=\mathrm{axl}(\mathrm{Res}^{\mathrm{ex}}(H,A^{\mathrm{ex}})) \tag{73}$$

DOI: 10.1002/nme

similar to (61) apart from the modified right-hand side whence the searched differential is obtained as $DA^{\mathrm{ex}}(B).H = \mathrm{anti}(x(H))$.

This result is the basis for a fully algorithmical treatment of the consistent linearization of the consistent weak form (29). However, the resulting algorithmic tangent is a cumbersome expression and is, therefore, not listed here. Moreover, our numerical experience showed that applying the consistent linearization has no pay off compared with a numerical tangent.

5. NUMERICAL EXAMPLES

In the remaining of this text we shall demonstrate the special features of our model by some illustrative examples. The material data of all models are summarized in Table I. Furthermore, let us mention that the viscosity parameter η controls the convergence of the rotational update (15) as shown in Section 4. It needs to fulfill the stability condition (40) but is arbitrary otherwise and has no actual influence on the material's response. Therefore, we do not list η as a material parameter but set it here and below to be $\eta = 0.01\,\mathrm{MPa\,s}$.

5.1. Rectangular sheet

At first we compute the bending of a dead-loaded sheet made of a relatively hard synthetic polymer. The midsurface $m(x, y)$ of the $40 \times 5\,\mathrm{mm}$ sheet is discretized with a regular triangulation of 1600 elements, $u_h \in \mathscr{P}_1(\mathscr{T})$. The membrane is completely fixed at the left boundary (where $x = 0$, see Figure 3(a)), constrained in the y-direction along its sides parallel to the x-axis and constrained in the vertical z-direction at the right boundary. Clearly, by nature of the model only the displacement can be constrained along the boundaries, cf. Remark 2.3.

A volumetric load (corresponding to a dead load) is applied on the sheet within $t_{\mathrm{load}} = 100\,\mathrm{s}$. Then, within 1000 s the right boundary is moved to the left, i.e. a displacement $u_x(t) = -\bar{u} \cdot (t - t_{\mathrm{load}})$ is prescribed with maximal displacement $\bar{u} = 8\,\mathrm{mm}$. After that period of time load and displacement are kept constant and the material starts to relax. In Figure 3(b)–(d) the initial and the deformed state of the sheet are displayed for different times of relaxation. In the beginning we clearly observe a bent sheet. Owing to energy minimization the rotations relax and finally run into one (central) kink.

The specific feature of the model to result in kinks of the membrane's mid-surface is a direct consequence of the completely neglected bending stiffness in the presented model. Discontinuities of rotations R along the finite element edges are a valid solution of the discrete problem (20). As outlined previously, this is not a shell-like theory of thin continua but the model is capable of representing the essential features of gossamer structures undergoing large deformations! Furthermore, results computed in that way are to a certain extent mesh dependent since the model is able

Table I. Material data and membrane thickness of the examples.

	μ (MPa)	λ (MPa)	ρ (kg/m^3)	h
Hard synthetic sheet (Section 5.1)	26 316	51 084	2.7	0.1 mm
Soft elastic foil (Section 5.2)	1358	2036	—	1 mm
Elastic Kapton foil (Section 5.3)	1358	2036	1.5	25 µm

DOI: 10.1002/nme

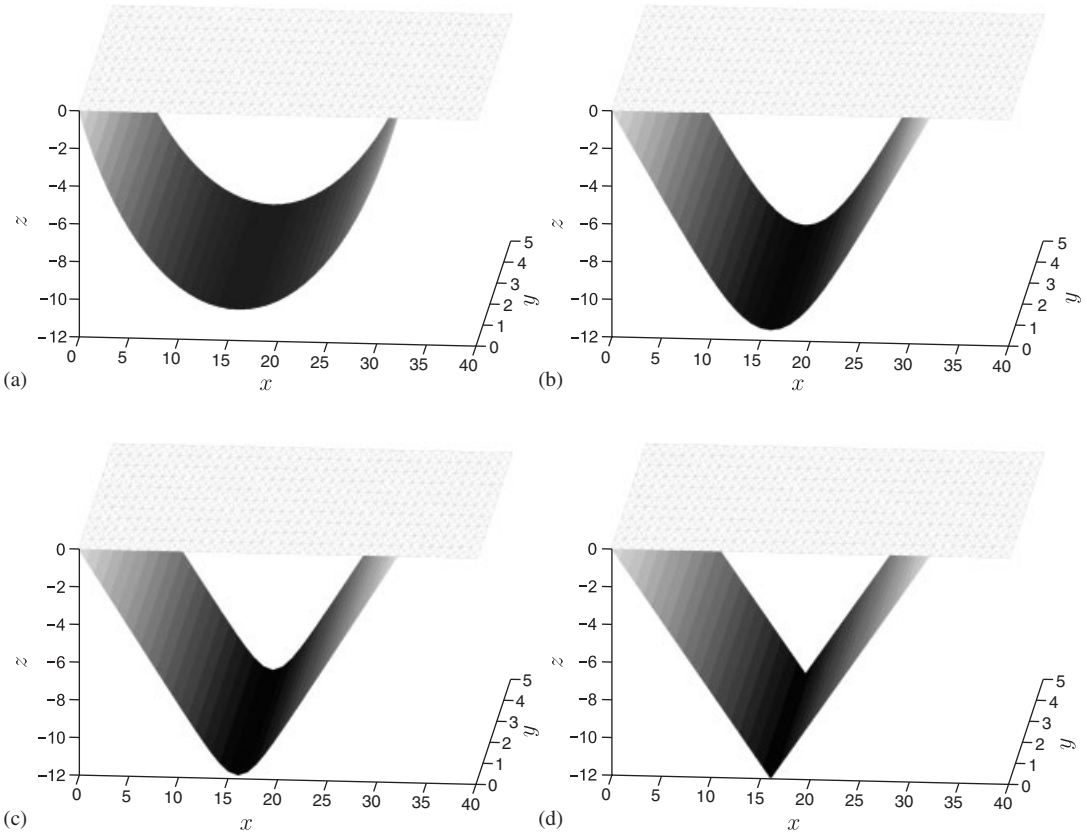

Figure 3. Initial and deformed state of a hard sheet loaded by dead load and subjected to in-plane displacement of one side after different time periods of relaxation. A relaxation time of 5000 s corresponds practically to the case of Remark 2.3, Equation (11): (a) no relaxation; (b) relaxation time 500 s; (c) relaxation time 1000 s; and (d) relaxation time 5000 s.

to kink only along the finite element boundaries. The regular triangulation in Figure 3 obviously allows for a straight central kink but variations of the mesh gave, provided that they were sufficiently fine, basically the same result.

5.2. Wrinkling of a thin foil

Let us now apply our model to the problem of an elastic foil under pressure load. The square foil has a side length of 2 m and a thickness of 1 mm; we think of a gossamer material like Kapton foil. The foil lays on a 1.2×1.2 m square obstacle (think of cloths on a table) and only the unsupported part of it can deform. The foil is loaded from above with a pressure of $p_0 = 0.75$ MPa. The initial situation is displayed in Figure 4(a). For the reason of symmetry only one quarter of the unsupported part is meshed with 6144 triangular elements. The displacements are constrained along the obstacles's edge and, moreover, symmetry conditions apply.

DOI: 10.1002/nme

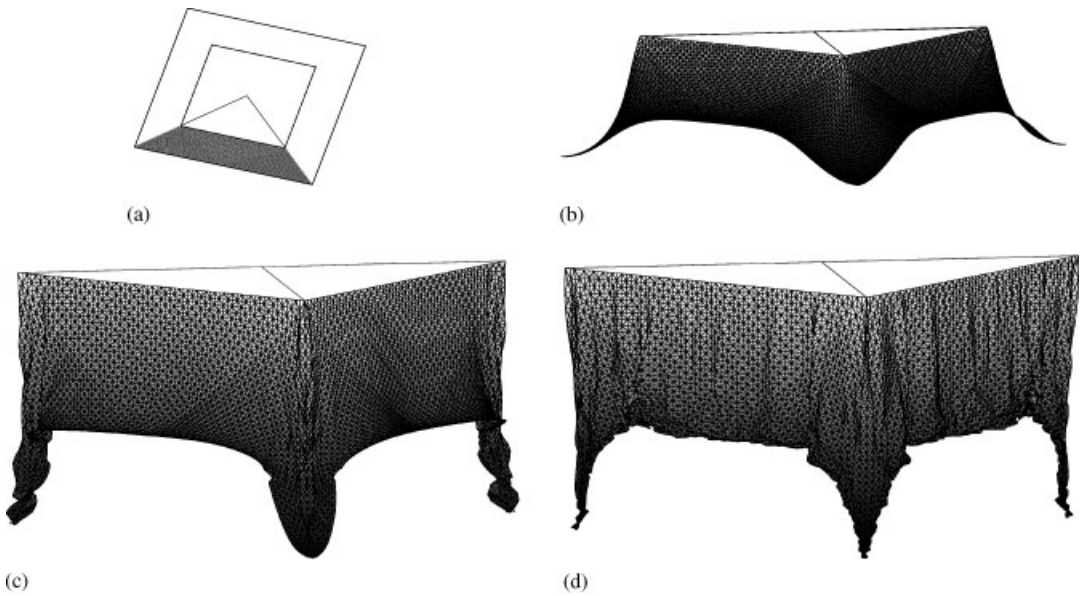

Figure 4. Wrinkling of a foil blown over a square obstacle: (a) computed model; (b) $p(t)=0.5p_0$; (c) $p(t)=p_0$, no relaxation; and (d) $p(t)=p_0$, relaxed state.

The computation started with a plane initial placement, the pressure is applied within 100 time steps of 10 s. Two intermediate states as well as the final deformation are displayed in Figure 4(b)–(d). The computed results are reflected on a symmetry axis and pictured for all models from the same point of view. Starting with the initial situation we observe a downward folding of the model. Because the membrane cannot handle a significant compressive stress it starts to fold at the corner sides of the foil under further rising of the pressure. Relaxing this state (and keeping the pressure constant) results in kinks along these sides.

Thinking of a typical wrapping foil, the observed pattern of wrinkles and folds seems realistic and the example nicely illustrates that a common limitation of many finite element analysis programs, namely, the inability to handle tensionless states of a membrane-like structure is not encountered here.

5.3. Twisting a band of elastic foil

Finally, we analyze the membrane's stress state turning a band of Kapton foil upside down. To this end a 100×400 mm strip of thin foil (with material data from [25], see Table I) is discretized. The band is stretched by 25% in the axial direction and both ends are turned against each other by 180°. The deformed membrane is shown in Figure 5; the black lines mark the controlled boundaries. (The finite element triangulation has 16 384 elements and is too dense to be displayed.) Along the marked edges the band is held tight and the displacements are prescribed resulting in a twisted stretch of the band. The deformation is computed in 30 time steps; the final (relaxed) state is reached within 10 additional time steps. The average band thickness reduces from initially 0.25 to 0.241 mm in the final state.

DOI: 10.1002/nme

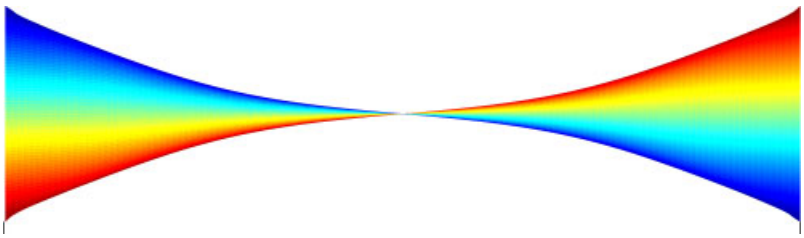

Figure 5. Twisted and stretched band of Kapton foil.

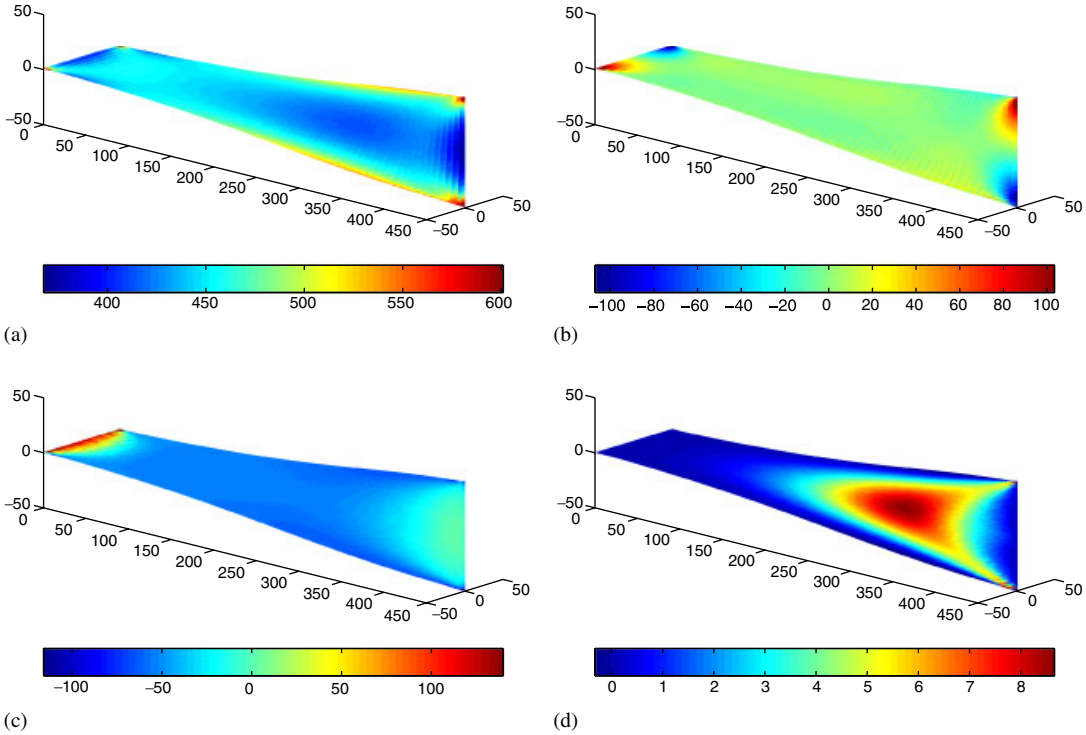

Figure 6. Axial stress, in-plane shear stress and in-plane and out-of-plane nominal stress components in the twisted foil strip: (a) axial stress component S_{11}; (b) shear stress component S_{12}; (c) nominal stress component S_{22}; and (d) nominal stress component S_{33}.

As Figure 5 shows, the presented membrane model is capable of *exactly* capturing such large deformation states. The only drawback to mention here is the relatively slow convergence of the equilibrium iteration; depending on the criteria to stop the iteration several numbers of Newton steps may be necessary. One reason for that may be the previously mentioned error of logarithmic and exponential mapping routines but more significant seems the fact that the linearization of the discretized weak form with respect to the deformation (which is performed here numerically) gives not the precise consistent tangent. Since by linearization w.r.t. the full gradient F^n the evolution of rotations, precisely, the increment of $\varrho_m R_3$ is not fully taken into account, the resulting tangent

DOI: 10.1002/nme

may deviate from an exact (but unknown) linearization. This, in turn, slows down convergence to the equilibrium solution in particular for large rotations.

Figure 6 illustrates the resulting stress state in the twisted band. Here, for the purpose of illustration, only one half of the band is computed and twisted by 90°, displayed are the components of the first Piola–Kirchhoff stress tensor (8). Evidently, the dominating stress component is the nominal stress in axial direction S_{11} with average values of 450 MPa and maxima along the boundaries. Shear stress S_{12} and the nominal out-of-plane stresses S_{33} are close to zero; only as a result of the clamped edges do we observe such stress components [26].

6. SUMMARY

In this paper we proposed a geometrically exact model for gossamer structures undergoing large deformations. Contrary to many other formulations the underlying theory of a thin membrane with viscoelastic transverse shear resistance is well posed even in a tensionless membrane state. A key feature of the model is an evolution equation for an independent field of rotations. These rotations adjust viscoelastically to the actual continuum rotations. A time discretization of the model is performed whereby the evolution equation for the rotations is locally integrated with an exponential update algorithm. By means of numerical studies the convergence of the proposed scheme is validated.

Numerical examples illustrate that in our model a common limitation of standard solution procedures, namely the inability to handle a locally slack membrane state is not encountered. The membrane model incorporates full geometric non-linear capabilities; only for simplicity we presume it to be initially plane. Note that the model is *not* restricted to such a plane initial state, an extension to curved structures is straightforward and, together with an extension to irreversible material behavior, subject of ongoing work. Typical applications of the model we have in mind are very thin sheets with negligible bending stiffness, e.g. synthetic foil, thin fabric or tissue.

ACKNOWLEDGEMENTS

The initial idea of this paper was conceived in the academic year 2001/2002 while both authors held a visiting faculty position under the ASCI program in Michael Ortiz group at the California Institute of Technology, Graduate Aeronautical Laboratories. We would like to thank Michael Ortiz for his kind hospitality.

REFERENCES

1. Ramm E, Wall WA. Shell structures—a sensitive interrelation between physics and numerics. *International Journal for Numerical Methods in Engineering* 2004; **60**:381–427.
2. Ciarlet PG. *Introduction to Linear Shell Theory* (1st edn). Series in Applied Mathematics. Gauthier-Villars: Paris, 1998.
3. Ortiz M, Gioia G. The morphology and folding patterns of buckling-driven thin-film blisters. *Journal of the Mechanics and Physics of Solids* 1994; **42**:531–559.
4. Jenkins CHM. *Gossamer Spacecraft*: *Membranes and Inflatable Structures Technology for Space Applications.* American Institute of Aeronautics and Astronautics: New York, 2001.
5. Steigmann DJ. Tension-field theory. *Proceedings of the Royal Society of London*, *Series A* 1990; **429**:141–173.
6. Wagner H. Ebene Blechwandträger mit dünnem Stegblech. *Zeitschrift für Flugtechnik und Motorluftschiffahrt* 1929; **20**:8–12.

DOI: 10.1002/nme

7. Reissner E. On tension field theory. *Proceedings of the 5th International Congress on Applied Mechanics*, vol. 5, 1938; 88–92.
8. Pipkin AC. Relaxed energy densities for large deformations of membranes. *IMA Journal of Applied Mathematics* 1994; **52**:297–308.
9. Le Dret H, Raoult A. The membrane shell model in nonlinear elasticity: a variational asymptotic derivation. *Journal of Nonlinear Science* 1996; **6**:59–84.
10. Roddeman D. The wrinkling of thin membranes: part I—theory. *Journal of Applied Mechanics* 1987; **54**:884–887.
11. Roddeman D. Finite element analysis of wrinkling membranes. *Communications in Applied Numerical Methods* 1991; **7**:299–307.
12. Neff P. A geometrically exact viscoplastic membrane-shell with viscoelastic transverse shear resistance avoiding degeneracy in the thin-shell limit. Part I: The viscoelastic membrane-plate. *Zeitschrift Angewandte Mathematik Physik* 2005; **56**(1):148–182. DOI: 10.1007/s00033-004-4065-0(Preprint 2337, http://wwwbib.mathematik.tu-darmstadt.de/Math-Net/Preprints/Listen/pp04.html).
13. Neff P. Finite multiplicative plasticity for small elastic strains with linear balance equations and grain boundary relaxation. *Continuum Mechanics and Thermodynamics* 2003; **15**(2):161–195.
14. Neff P. Local existence and uniqueness for a geometrically exact membrane-plate with viscoelastic transverse shear resistance. *Mathematical Methods in the Applied Sciences* 2005; **28**:1031–1060. DOI: 10.1002/mma.597 (Preprint 2364, http://wwwbib.mathematik.tu-darmstadt.de/Math-Net/Preprints/Listen/pp04.html).
15. Le Dret H, Raoult A. From three-dimensional elasticity to nonlinear membranes. In *Asymptotic Methods for Elastic Structures, Proceedings of the International Conference*, Ciarlet PG, Trabucho L, Viano JM (eds). Walter de Gruyter: Berlin, 1995.
16. Miara B. Nonlinearly elastic shell models: a formal asymptotic approach. I. The membrane model. *Archive for Rational Mechanics and Analysis* 1998; **142**:331–353.
17. Ciarlet PG, Sanchez-Palencia E. Ellipticity of bending and membrane shell equations. In *Asymptotique Methods for Elastic Structures, Proceedings of the International Conference*, Ciarlet PG, Trabucho L, Viano JM (eds). Walter de Gruyter: Berlin, 1995.
18. Le Dret H, Raoult A. The nonlinear membrane model as a variational limit of nonlinear three-dimensional elasticity. *Journal de Mathématiques Pures et Appliquées* 1995; **74**:549–578.
19. Haseganu E, Steigmann DJ. Analysis of partly wrinkled membranes by the method of dynamic relaxation. *Computational Mechanics* 1994; **14**:596–614.
20. Higham NJ. Computing the nearest symmetric positive semi-definite matrix. *Linear Algebra and its Applications* 1988; **103**:103–118.
21. Holzapfel G. *Nonlinear Solid Mechanics.* Wiley: New York, 2000.
22. Carstensen C, Weinberg K. An adaptive nonconforming finite element method for Reissner–Mindlin plates. *International Journal for Numerical Methods in Engineering* 2003; **56**:2313–2330.
23. Weinberg K. An adaptive finite element approach for a mixed Reissner–Mindlin plate formulation. *Computer Methods in Applied Mechanics and Engineering* 2001; **190**(37–38):4999–5008.
24. Hofmann KH, Morris SA. *The Structure of Compact Groups.* Studies in Mathematics. deGruyter: Berlin, 1998.
25. Wong YW, Pellegrino S. Wrinkled membranes. In *Textile Composites and Inflatable Structures*, Onate E, Kröplin B (eds). CIMNE: Barcelona, 2003.
26. Carstensen C, Weinberg K. Calculating the energy-norm FEM-error for Reissner–Mindlin plates without known reference solution. *Computational Mechanics* 2000; **26**(6):566–570.